https://doi.org/10.5194/wes-2024-119
Preprint. Discussion started: 2 October 2024

eawe european academy of wind energy
Open Access WIND ENERGY SCIENCE DISCUSSIONS

Tall Wind Profile Validation Using Lidar Observations and Hindcast Data

Etienne Cheynet[1,*], Jan Markus Diezel[1,*], Hilde Haakenstad[2], Øyvind Breivik[2,3], Alfredo Peña[4], and Joachim Reuder[1]

[1]Bergen Offshore Wind Centre (BOW) and Geophysical Institute, University of Bergen, Norway
[2]Norwegian Meteorological Institute, Norway
[3]Geophysical Institute, University of Bergen, Norway
[4]DTU Wind and Energy Systems, Technical University of Denmark, Denmark
[*]These authors contributed equally to this work.

Correspondence: Etienne Cheynet (etienne.cheynet@uib.no)

Abstract. The development of large offshore wind turbines and airborne wind energy (AWE) systems requires reliable wind speed datasets at heights far above the atmospheric surface layer. Traditional measurement approaches, primarily reliant on met-masts, fall short of addressing the needs of modern wind turbine design and AWE systems development. In this study, we validate three different model-based datasets, namely the 3-km Norwegian Hindcast archive (NORA3), the New European Wind Atlas (NEWA), and ERA5 using Doppler wind lidar data from several locations in Norway and the North Sea. The validation focuses on altitudes from 100 to 500 m above ground, covering the operational range of large wind turbines and AWE systems. Our findings indicate that ERA5 and NORA3 perform remarkably well in offshore locations, with ERA5 showing the closest correlation to lidar data up to 200 m. NORA3 outperforms the other two models in two coastal and one complex terrain sites. Finally, an increasing agreement between the models and lidar measurements with height suggests that model-based datasets can be valuable for AWE systems research and development.

1 Introduction

The hub height and rotor diameter of offshore wind turbines (OWTs) have been continuously increasing over the past 20 years (Jahani et al., 2022; Jiang, 2021), reaching up to 150 m and over 200 m, respectively. This trend is driven by the need to capture stronger and steadier winds to reduce the overall levelized cost of energy (Wiser et al., 2021). In the near future, the top tip height of offshore wind turbines may reach almost 300 m above the surface.

Since the 2010s, commercial airborne wind energy (AWE) systems have demonstrated notable advancements (Vermillion et al., 2021; Fagiano et al., 2022; Eijkelhof and Schmehl, 2022). Prototypes of AWE systems with capacities exceeding 600 kW (Vermillion et al., 2021) and potentially developing into multi-megawatt have been proposed (Kruijff and Ruiterkamp, 2018). However, AWE systems remain in the early stage of development compared to offshore wind turbines. Recent efforts in performance assessment have relied mainly on ground-generation AWE systems, which is the most mature technology at the

https://doi.org/10.5194/wes-2024-119
Preprint. Discussion started: 2 October 2024

eawe european academy of wind energy
Open Access WIND ENERGY SCIENCE DISCUSSIONS

moment (Vermillion et al., 2021). Such studies used simulated wind speed profiles, with optimal operating heights for AWE systems identified between 200 and 600 m above the surface (Sommerfeld et al., 2019b).

Traditional approaches for estimating mean wind speed profiles rely on mast-based measurements, which are primarily applicable to studying the atmospheric surface layer (ASL). The ASL constitutes approximately the lowest 10% of the atmospheric boundary layer (ABL). Under neutral and unstable atmospheres, the depth of the ASL ranges from 50 m to 100 m offshore and can extend up to 200 m onshore (Pal and Lee, 2019; Davis et al., 2020, 2022). Under a stable atmosphere, the ASL is shallow, with a depth sometimes close to a dozen metres (Mason and Derbyshire, 1990). Traditional logarithmic and power-law mean wind speed profiles, such as those used in IEC 61400-1 (IEC, 2005), are limited to the ASL and are likely inadequate for wind turbine design with hub heights of 150 m or more (Tieo et al., 2020; Cheynet et al., 2024). For wind resource assessment, the height-dependent Weibull parameters (Kelly et al., 2014) require the characterization of wind speed profiles above 200 m. Therefore, the development of both AWE systems and future OWTs necessitates information on the mean wind speed at heights several hundred meters above the surface.

Tall wind profiles, as defined here, cover the entire atmospheric boundary layer (ABL) or at least the initial 500 m above the surface. Traditional tall masts often fall short of this definition, as they are typically lower than 100 m. Only a limited number of masts exceeding 200 m exist globally (Ramon et al., 2020), and these are exclusively onshore masts (table 1). Although tall-wind speed profiles can also be collected using manned aircraft (e.g. Zemba and Friehe, 1987) or drones (Egger et al., 2002; Reuder et al., 2009; Palomaki et al., 2017; Shimura et al., 2018), this approach has not been adopted for wind resource assessment, which requires several years of data. Therefore, the characterization of mean wind speed profiles above the marine surface layer is a major challenge (Shaw et al., 2022; Veers et al., 2019).

Commercial Doppler wind lidar (DWL) profilers measure wind speed and direction up to approximately 300 m above the surface (Peña et al., 2009). They operate using fixed beams at predetermined angles with modes like Doppler beam swinging (DBS) or velocity azimuth display, showing good performance against tall met masts (Knoop et al., 2021). Commercial DWL profilers, both ground-based and mounted on fixed platforms, have been used in wind energy research for over a decade, both onshore (Smith et al., 2006; Kumer et al., 2016) and offshore (Peña et al., 2009; Peña et al., 2015). In the 2010s, floating wind lidar profilers deployed on buoys (Gottschall et al., 2017; Peña et al., 2022) and ships (Rubio et al., 2022) began to complement traditional met-masts, offering cost reductions (Krishnamurthy et al., 2013).

Most commercial DWL wind profilers are still limited to studying the mean wind flow in the first 300 m above the surface. Scanning DWLs possess a more powerful laser than lidar profilers, allowing them to collect data up to 3 km under good aerosol conditions (Kumer et al., 2014). This technology, used in atmospheric research for over two decades (Pichugina et al., 2012; Banta et al., 2013; Dias Neto et al., 2023), saw commercial adoption mainly in the early 2010s (Vasiljevic, 2014; Kumer et al., 2014). Scanning DWLs with hemispherical scanning capabilities can adjust both azimuth and elevation angles and can be set to mimic profiler modes for direct atmospheric profiling. Despite their potential, scanning lidars are often underutilized in developing airborne wind energy systems (AWE systems) or next-generation multi-megawatt offshore wind turbines. Notable examples of wind speed data collection with such instruments for tall wind profile analysis include Kumer et al. (2014) in coastal

https://doi.org/10.5194/wes-2024-119
Preprint. Discussion started: 2 October 2024

eawe european academy of wind energy
Open Access WIND ENERGY SCIENCE DISCUSSIONS

Table 1. Some of the tall met masts with top height above 200 m documented in Ramon et al. (2020) and in the scientific literature. None of these masts are offshore. The list includes both current and former masts.

Tower name	Top sensor (m)	Country
Walnut Grove	488	USA
Park Falls	396	USA
West Branch	379	USA
South Carolina	329	USA
Beijing Meteorological Tower	325	China
Gartow	341	Germany
Obninsk	301	Russia
Boulder Observatory	300	USA
Boseong	300	South Korea
Hamburg	280	Germany
Steinkimmen	252	Germany
Østerild	250	Denmark
KIT	200	Germany
Cabauw	200	Netherlands

terrain, Reuder et al. (2024) at the FINO1 offshore platform, Päschke et al. (2015) and Sommerfeld et al. (2019a) in Germany or Mariani et al. (2020) in the Arctic.

Recently, open-source datasets from wind hindcast or reanalysis databases such as the 3-km Norwegian Hindcast archive (NORA3) (Haakenstad et al., 2021), the New European Wind Atlas (NEWA) (Hahmann et al., 2020), and ERA5 (Hersbach et al., 2020) have provided model-based wind speed profiles within the first 500 m above the surface. NORA3 and ERA5 appear adequate for wind resource assessment and structural design, for which a climatological description of wind conditions over the first 500 m spanning at least 30 years is necessary. Note that NEWA falls slightly short of this definition, as it only covers 10 years of data. Although these databases can complement in-situ measurements, they require proper validation for wider use in wind energy. Portions of these databases have undergone validation against near-surface measurements (e.g. Ramon et al., 2019), mast measurements at levels below 100 m (Olauson, 2018; Jourdier, 2020; Solbrekke et al., 2021; Cheynet et al., 2022), or tall-masts measurements up to 200 m (Knoop et al., 2020; Gualtieri, 2021). Additional validation has been conducted using Doppler wind lidar technology for heights up to 300 m above the surface (Pronk et al., 2022; Hallgren et al., 2024). The comparison of lidar wind profiles with hindcast or reanalysis products at higher altitudes remains, however, limited. This motivates our study in an attempt to bridge this identified knowledge gap.

In this study, we validate datasets from the ERA5 global reanalysis, NEWA and NORA3 against in-situ measurements from DWL systems across diverse terrain locations in the North Sea and Norway to evaluate their accuracy in capturing tall wind speed profiles. We also aim to quantify the performance of these databases as a function of altitude using multiple error metrics.

https://doi.org/10.5194/wes-2024-119
Preprint. Discussion started: 2 October 2024

eawe european academy of wind energy
Open Access WIND ENERGY SCIENCE DISCUSSIONS

The selection of different sites offers the possibility to examine the impact of topography on local wind conditions. Thus, the novelty of this study resides in both, the collection of wind speed data in the entire ABL, and the inter-comparison of various hindcast or reanalysis wind databases at altitudes up to 500 m, which has yet to attract significant attention. Moreover, this study expands the validation to include the capacity factor for modern offshore wind turbines and AWE systems. This research is believed to be valuable to both wind energy and wind engineering, as tall wind speed profiles can be used for both wind resource assessment and wind loading on structures (Kent et al., 2018).

This study is organised as follows: section 2 introduces the datasets extracted from the ERA5, NORA3 and NEWA databases, as well as the DWL data. Section 3 presents the metrics used for the error analysis and the data processing to collocate the modelled and measured data in space and time. Section 4 studies the influence of the choice of the site and the height on the errors between the wind atlases and in-situ data. Our findings underscore ERA5's reliability offshore, especially above 100 m. However, in coastal locations and complex terrains, regional model-based datasets become necessary. In some instances, microscale wind models may even be needed to more accurately capture the local wind conditions. Section 4 presents also the influence of the choice of the wind atlas on the estimation of the capacity factor of a modern wind turbine and an airborne wind energy system. Finally, section 5 discusses the need for more powerful DWL profilers and the complementary role of mesoscale and microscale simulations for improved wind resource assessment.

2 Data collection and wind models

2.1 Model data

A state-of-the-art wind atlas is defined herein as a climate dataset that provides the mean wind speed and mean wind direction at multiple heights above the surface. It provides a horizontal spatial resolution on the kilometre scale, a time resolution of 1 h or finer, and temporal coverage of at least 10 years. The definition of a wind atlas employed here relates to a hindcast or reanalysis database that is usable for wind resource assessment or the design of wind energy systems, including extreme value analysis. In this context, both NEWA and NORA3 qualify as state-of-the-art wind atlases. They are regional downscaling products of the ERA5 reanalysis (Hersbach et al., 2020), covering overlapping areas in Europe (fig. 1). Consequently, ERA5 data are also included in this analysis. Although wind atlases are sometimes defined as databases with microscale spatial resolution finer than 1 km, we choose to adopt a broader definition that includes model-based wind data with a kilometre-scale resolution.

The ERA5 reanalysis product from the European Centre for Medium-Range Weather Forecasts (ECMWF) superseded ERA-Interim in 2019 (Dee et al., 2011). ERA5 offers climate data with global coverage, a horizontal spatial resolution of approximately 31 km and a hourly output, extending from 1940 onward. As a reanalysis product, ERA5 uses a 4D-Var data assimilation scheme within a 12-hour assimilation window, incorporating both in-situ measurements and satellite observations (Hersbach et al., 2020). The ERA5 temporal resolution and extensive temporal coverage are valuable for wind energy research globally (Olauson, 2018), including the analysis of annual and decadal wind variability and potential trends due to climate change (Chen, 2024; Antonini et al., 2024; Martinez and Iglesias, 2024). Researchers and engineers in the wind energy sector increasingly rely on ERA5 for both historical analysis and future project planning (Olauson, 2018; Gualtieri, 2021; Hayes et al.,

https://doi.org/10.5194/wes-2024-119
Preprint. Discussion started: 2 October 2024

eawe european academy of wind energy
Open Access WIND ENERGY SCIENCE DISCUSSIONS

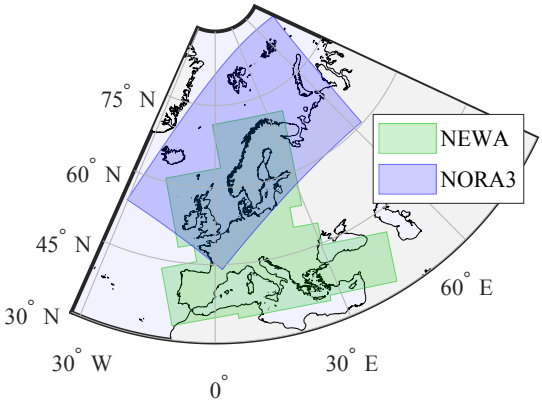

Figure 1. Illustration of the regions covered by NEWA and NORA3. ERA5 has global coverage and is thus not shown here.

2021). This reliance underlines the importance of accurate, high-resolution climate reanalyses in advancing renewable energy technologies.

NEWA is an open-access European wind atlas released in 2019 and developed through collaboration among 30 European academic and industrial partners (Hahmann et al., 2020; Dörenkämper et al., 2020). NEWA uses the Weather Research and Forecasting (WRF) model and utilizes the ERA5 reanalysis as forcing, without further data assimilation. NEWA aims to provide a detailed wind climatology of Europe with a spatial resolution of approximately 3 km and a temporal resolution of 30 min. In this study, data on mean wind speed and direction from NEWA were retrieved from https://map.neweuropeanwindatlas.eu/ for eight altitudes, ranging from 10 m to 500 m above sea level (asl).

NORA3 is a regional downscaling of the ERA5 reanalysis and utilizes the HARMONIE-AROME non-hydrostatic regional numerical weather prediction model for its production (Haakenstad et al., 2021). The downscaling consists of nine-hour short integration runs initiated every six hours, employing the last run as the initial state for the new cycle. Surface observations in the CANARI-OI-Main assimilation system adjust the first-guess (Giard and Bazile, 2000; Taillefer, 2002), with ERA5 forcing applied in the free atmosphere following the boundary relaxation method (Radnoti, 1995; Termonia et al., 2018). NORA3 is built on NORA10's legacy, which has been used by the offshore industry in the North Sea for over a decade (Furevik and Haakenstad, 2012) and refines the description of the wind condition provided by NORA10 (Haakenstad et al., 2021). Validations of the NORA3 database against atmospheric data include comparisons with wind measurements from oil and gas platforms, as well as offshore masts in the North Sea and Norwegian Sea (Solbrekke et al., 2021). NORA3 provides wind data once per hour with a 3 km spatial resolution across 65 layers in a hybrid sigma-pressure coordinate scheme. A specific subset, released in 2021 by the Norwegian Meteorological Institute, has been selected for this study. This subset presents mean wind speed and direction data at seven heights, from 10 to 750 m asl. Table 2 details the metadata for the different models, illustrating the variability in spatial and temporal resolutions, as well as available height levels above 100 m among NORA3, NEWA, and ERA5.

https://doi.org/10.5194/wes-2024-119
Preprint. Discussion started: 2 October 2024

eawe european academy of wind energy
Open Access WIND ENERGY SCIENCE DISCUSSIONS

Table 2. Metadata of the wind atlas data sets. Only z-levels above 100 m are shown hereinafter. ERA5 data were collected using the 100 m z-level with additional height levels retrieved using pressure levels and the geopotential height. Δh is the horizontal spatial resolution and Δt is the temporal resolution in minutes.

	Δh (km)	Δt (min)	z-levels (m)
NORA3	3	60	100, 250, 500, 750
NEWA	3	30	100, 150, 200, 250, 500
ERA5	31	60	100, geopotential heights

2.2 The measurement sites

The measurement data were collected by DWL instruments within the area covered by ERA5, NORA3, and NEWA (fig. 2). Two lidar campaigns were conducted in the marine atmospheric boundary layer at the FINO1 and FINO3 locations, two other campaigns took place in coastal sites (Sola and Lista airports in Norway) and one in complex terrain (Bjerkreim, Norway). Offshore sites refer here to locations situated in open waters, typically over a few dozen kilometres from the coast, while coastal sites refer to flat onshore locations a few kilometres from the shoreline. Complex terrain refers to areas characterized by heterogeneous topography, such as hills or mountains. Table 3 summarises the locations and measurement periods of the five campaigns selected for the validation of wind atlases. The diversity of locations, comprising two offshore, two coastal, and one in complex terrain, offers additional possibilities to assess the performances of the wind atlases at higher altitudes. This study uses lidar data as reference datasets, given their suitability for capturing wind speed data across the entire ABL. Data availability above 500 m decreases due to factors such as low clouds and low aerosol content, as illustrated in fig. 3. This figure defines data availability as a function of the carrier-to-noise (CNR) ratio. More specifically, missing data or data with a CNR under -27.5 dB for the scanning lidar instrument and under -22 dB for the DWL profiler are dismissed. The threshold value for the scanning lidar is lower than the value of -22 dB used in Peña et al. (2015), which is usually applied to DWL profilers. However, a lower threshold can be applied for scanning Doppler wind lidar (Cheynet et al., 2017). For simplicity, specific methods, e.g. those presented by Beck and Kühn (2017); Valldecabres et al. (2018); Cheynet et al. (2021) or Duscha et al. (2023) to rescue data with even lower CNR are not considered here, as only the mean wind speed was of interest.

The measurement principle involves all lidar devices operating in DBS mode. This mode reconstructs horizontal wind speed and direction from the radial velocities of four beams, incorporating two volume averaging effects: one over the range gate length of each beam and another across the horizontal area over the lidar increasing with height, defined by the four beams at a given opening angle of typically 30 degrees. The DBS mode assumes horizontal homogeneity of the mean flow, a condition typically met in flat and homogeneous terrain but often violated in highly complex terrain (Pauscher et al., 2016) or near obstacles, such as in the wake of a wind turbine. As altitude increases, the flow tends to become more homogeneous and horizontal, making DBS scanning suitable for measuring tall wind speed profiles.

https://doi.org/10.5194/wes-2024-119
Preprint. Discussion started: 2 October 2024

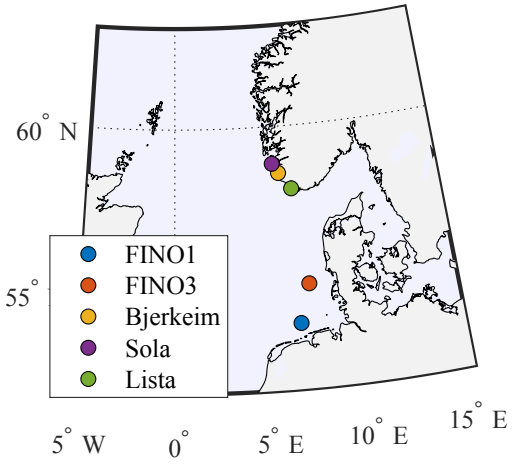

Figure 2. Location of the five measurement sites in the North Sea and along the Norwegian coast.

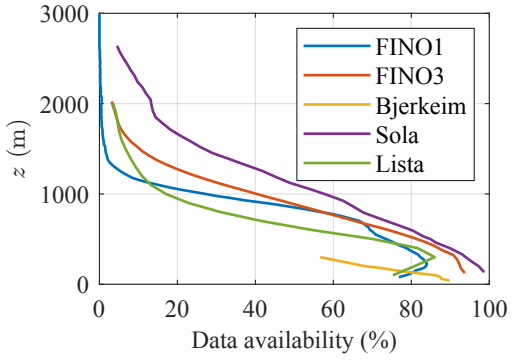

Figure 3. Data availability during the five measurement campaigns as a function of the altitude, based on the Carrier-to-Noise Ratio (CNR).

The first measurement campaign was conducted in Bjerkreim, Southwest Norway, from March to May 2010. The site, characterized by rocky terrain and sparse vegetation, presented a complex topography. A WindCube V1 DWL (Leosphere) was deployed to capture wind profiles at altitudes ranging from 40 m to 300 m above the surface. Approximately 799 hours of data were collected. The mean wind speed records were subsequently validated against sodar measurements taken 300 m away from the lidar's location.

The second measurement campaign, known as the LIdar MEasurement Campaign Sola (LIMECS) (Kumer et al., 2014), was conducted at Stavanger Airport Sola, Norway, from March to June 2013. The objective was to evaluate the capability of a long-range pulsed lidar instrument in measuring mean wind speed at altitudes beyond the reach of traditional meteorological masts. A first-generation WindCube 100S lidar was deployed, operating in DBS scanning mode and capturing wind profiles at a minimum height of 133 m above the surface. This campaign resulted in the collection of approximately 525 hours of data.

https://doi.org/10.5194/wes-2024-119
Preprint. Discussion started: 2 October 2024

Table 3. Metadata of datasets from five lidar measurement campaigns. The lidar range gate denotes the along-beam spatial resolution.

	FINO1	FINO3	Lista	Sola	Bjerkreim
Latitude (N)	54.015	55.195	58.104	58.885	58.595
Longitude (E)	6.588	7.158	6.631	5.631	5.955
Terrain Type	Offshore	Offshore	Coastal	Coastal	Complex
Device	Windcube 100S	WLS70	WLS70	Windcube 100S	WindCube V1
Start Date	01.06.2015	10.09.2013	20.11.2020	04.03.2013	30.03.2010
End Date	05.10.2016	06.10.2014	06.09.2021	30.06.2013	06.05.2010
Hours Collected	1353	7997	6912	525	799
Min height (m)	78	125	100	133	40
Max height (m)	3528	2025	2000	2641	300
Range Gate (m)	25	50	100	75	20

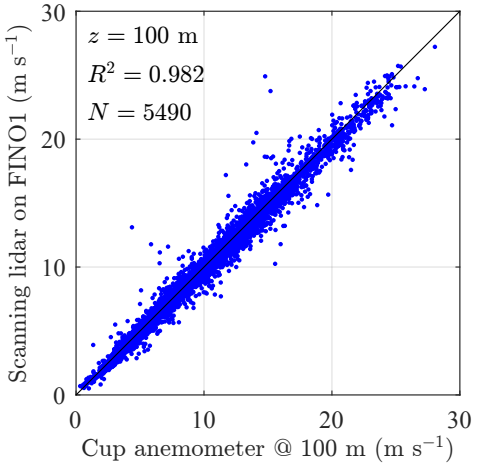

Figure 4. Comparison of 10-minute mean wind speed measurements recorded by the cup anemometer and the WindCube 100S at 100 m above sea level, collected between June 2015 and October 2016 during the OBLEX-F1 campaign at the FINO1 platform.

The lidar measurements were compared against radiosonde data, demonstrating a strong correlation with a Pearson coefficient $R > 0.95$, which improved with increasing altitude.

The third measurement campaign took place at the FINO3 offshore platform, located at $55.195°$N, $7.158°$E in the North Sea, approximately 80 km from the Danish coast. The platform hosted a WLS70 DWL profiler by Leosphere (Cariou et al., 2009) from August 2013 to October 2014. The lidar operated in DBS scanning mode with a scan angle of $14.7°$, resulting in the collection of approximately 7997 hours of data. The lowest measurement height, at 125 m above sea level (asl), ensured no significant mast-induced flow distortion. The collected wind speed and direction data were validated and detailed in Peña et al. (2015).

https://doi.org/10.5194/wes-2024-119
Preprint. Discussion started: 2 October 2024

eawe european academy of wind energy
Open Access WIND ENERGY SCIENCE DISCUSSIONS

The fourth measurement campaign was conducted at the FINO1 offshore platform, located at $54.014°$N, $6.587°$E in the southern North Sea, approximately 45 km north of Borkum Island, Germany. The platform hosted a Windcube 100S (Leosphere) long-range scanning DWL from 01 June 2015 to 05 October 2016 (Reuder et al., 2024). The lidar operated in DBS scan mode with a fixed elevation angle of $70°$, performing scans twice every hour to collect 10-minute mean wind speed profiles. A total of approximately 1353 hours of data were recorded, with the lowest measurement height at 78 m above the sea surface. A preliminary comparison with a reference cup anemometer mounted at the top of the FINO1 mast (100 m above the sea surface) showed excellent agreement, with a squared Pearson coefficient of 0.98, similar to results from a study conducted at the FINO3 platform (Peña et al., 2015). The lidar data collected at FINO1 are therefore considered reference data in this study (fig. 4).

The fifth measurement campaign took place at Farsund Airport (Lista, Norway) from November 2020 to September 2021, focusing on the study of the atmospheric boundary layer for airborne wind energy applications. A WindCube WLS70 lidar was deployed and operated in DBS mode with measurement heights ranging from 100 to 2000 m above the surface. This paper analyses nearly one year of wind speed records, resulting in approximately 6912 hours of data.

3 Methods

3.1 Error metrics

To quantify discrepancies between mean wind speed data obtained from lidar instruments and those predicted by wind atlases, four metrics are employed: the squared Pearson correlation coefficient (R^2), the bias, the Root-Mean-Square Error (RMSE), and the first Wasserstein distance, also known as the Earth Mover's Distance (EMD). The squared Pearson correlation coefficient (R^2) measures the linear correlation between the measured and modelled wind speeds. The bias quantifies the average difference between the predicted and observed values, providing a measure of systematic error and the Root-Mean-Square Error (RMSE) quantifies the average magnitude of the error. The EMD quantifies the dissimilarity between two probability distributions, making it well-suited for analysing wind atlases that represent the climatology of a site in terms of the probability distribution of mean wind speed and direction (Hahmann et al., 2020). For brevity, only the EMD equation is introduced, as the equations for the R^2 coefficient, RMSE, and bias are assumed to be familiar to the reader. For one-dimensional distributions, the EMD can be represented by the area between two cumulative distribution functions (CDFs), F_1 and F_2:

$$\mathrm{EMD} = \int_{-\infty}^{+\infty} |F_1(x) - F_2(x)| \, \mathrm{d}x. \tag{1}$$

3.2 Data preprocessing

The data preprocessing is similar for all campaigns: Hindcast data are initially interpolated from their original horizontal grid to the GPS coordinates of the lidar campaign locations at each vertical height level. The interpolation scheme follows the method described in Amidror (2002), specifically a linear scattered data interpolation, as the data from the wind atlases are not necessarily on a Cartesian grid.

https://doi.org/10.5194/wes-2024-119
Preprint. Discussion started: 2 October 2024

The datasets from NORA3 and NEWA are provided at specific height levels, whereas the ERA5 data were collected at five pressure levels (1000, 975, 950, 925, and 900 hPa), as well as at 10 and 100 m above the surface. The pressure levels were converted into geopotential height levels using the geopotential variable available in the ERA5 database. Although geopotential height slightly differs from geometric height, this study focuses on wind speed data within the first 500 m above the surface, where the approximation of geopotential height to geometric height is expected to be sufficiently accurate.

A linear interpolation method was employed for vertical spatial collocation between model and lidar data. Alternative non-linear interpolation schemes were also tested, such as spline, piecewise cubic Hermite interpolating polynomial methods, and the modified Akima method (Akima, 1974), but they yielded similar results while being less robust than the linear interpolation. Appendix A presents the error metrics quantified at specific heights and as vertical profiles using a non-linear regression. The non-linear regression shows minor differences in the error metrics compared to linear interpolation but does not change the conclusions of the study. The comparison in appendix A supports our decision to use linear interpolation for additional height levels in this study.

Following the spatial collocation, the model data were then temporally collocated with the lidar data. The lidar data consist of 10-minute averaged time histories, while the model data are provided at 60-minute or 30-minute resolutions. The first approach (Approach A) involves interpolating the model data to align with the 10-minute averages from the lidar. An alternative approach (Approach B) would be to interpolate the lidar data to an hourly timestep. However, Approach B is more complex than Approach A and did not yield significant differences. Therefore, for simplicity and to avoid overprocessing the data, Approach A was adopted. Finally, for the lidar data, the initial outlier detection and removal method, which relied on CNR threshold values of -27.5 dB for the scanning DWL and -22 dB for the DWL profiler, was found to be sufficiently effective, eliminating the need for additional outlier tests.

3.3 Power curves and capacity factor

This subsection outlines the methodology used to evaluate how different wind atlases influence the estimated capacity factors of wind turbines and AWE systems at the five selected sites. The turbines examined include a range of models from the NREL 5 MW with a 90 m hub height to the NREL 18 MW with a 156 m hub height, detailed in table 4. The power curves for these turbines are defined by a rated wind speed typically between 10 and 12 m s^{-1}, with a cut-in speed of 3 to 4 m s^{-1} and a cut-out speed of approximately 25 m s^{-1}.

The power curve for AWE systems depends on flight height and trajectory, complicating the estimation of annual energy production and capacity factors. To address this challenge, various approaches are possible, such as clustering methods for faster computation of AWES production (Schelbergen et al., 2020) or simplified power curves (Eijkelhof and Schmehl, 2022; Ranneberg et al., 2018). In this study, we opted to use simplified power curves as we focus primarily on validating tall wind speed profiles using scanning lidar instruments, without delving into AWE systems flight trajectory optimization. Two simplified power curves for AWE systems are considered: one developed for a 3 MW rigid body (Eijkelhof and Schmehl, 2022) and one for a smaller 100 kW AWE system (Ranneberg et al., 2018). The power curves of the 3 MW and 100 kW systems are displayed in the middle and bottom panels of fig. 5, respectively. These power curves represent a balance between simpler ones, such

https://doi.org/10.5194/wes-2024-119
Preprint. Discussion started: 2 October 2024

Table 4. Summary of wind turbine models tested with ERA5, NORA3, and NEWA datasets, available at https://nrel.github.io/turbine-models.

Model Name	Hub Height (m)	Rotor Diameter (m)
NREL 5 MW	90	126
Leanwind 8 MW	110	164
NREL 10 MW	119	198
DTU 10 MW	119	178
IEA 10 MW	119	198
IEA 15 MW	150	240
NREL 18 MW	156	263

as those used in Vos et al. (2024), where the rated power remains constant above the rated wind speed, and more advanced path-dependent approaches studied in Eijkelhof and Schmehl (2022) or Sommerfeld et al. (2023).

In the middle panel of fig. 5, we smoothed the 3 MW power curve using non-linear regression with smoothing splines, leading to cut-in and cut-out wind speeds of 9.0 and 29.9 m s^{-1}, respectively. These values slightly differ from those in the study by Eijkelhof and Schmehl (2022), which were based on ten optimized flight paths. Notably, we adopted a lower cut-in wind speed of 9 m s^{-1} compared to their 10 m s^{-1}, a distinction that may be significant in the North Sea where median wind speeds typically range between 9 and 10 m s^{-1} (Cheynet et al., 2024). The smoothed power curve for the 3 MW AWE system does not account for negative power output at the lowest wind speed of 8 m s^{-1} because it is assumed that the AWE system will not operate at such wind speeds. For the 100 kW AWE system, we averaged two power curves computed at 200 m and 300 m above the surface based on Ranneberg et al. (2018), resulting in a cut-in wind speed of 2 m s^{-1}, a cut-out wind speed of 20 m s^{-1} and a rated wind speed of 7.5 m s^{-1}. Unlike a wind turbine, the rated power in this curve decreases with increasing wind speed due to the retraction phase, which leads to a loss of power (Eijkelhof and Schmehl, 2022). Note that because the two power curves for the AWE system display significantly different rated wind speeds, they are likely to lead to large differences in capacity factors, which is discussed in section 4.

In this study, the wind speed values used for the power curve of the AWE systems are based on the median of mean wind speeds recorded at altitudes between 200 and 500 m. A similar approach was adopted in Vos et al. (2024) using a single height of 350 m above the surface. However, at sites with complex terrain, such as Bjerkreim, we limited measurements to between 200 and 300 m due to lidar profiler constraints. The choice of averaged wind speed values from altitudes between 200 and 500 m serves a dual purpose. Firstly, these altitudes align with the operational heights of large AWE systems (Eijkelhof and Schmehl, 2022). Secondly, this selection facilitates the approximation of capacity factors for AWE systems, avoiding the time-consuming task of calculating an optimal flight path for each wind speed profile.

https://doi.org/10.5194/wes-2024-119
Preprint. Discussion started: 2 October 2024

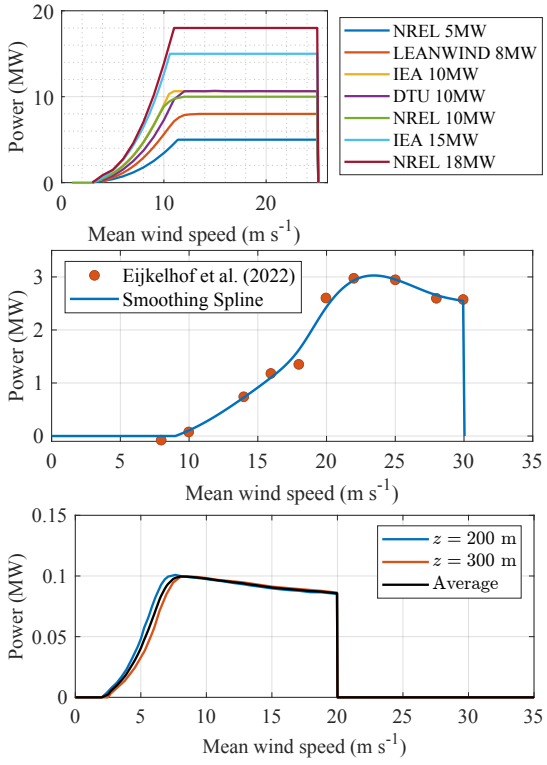

Figure 5. Power curves of the wind turbines investigated (top panel), the 3 MW airborne wind energy system presented in Eijkelhof and Schmehl (2022) (middle panel) and power curves for the 100kW AWES from Ranneberg et al. (2018) with averaged operating value between 200 and 300 m (bottom panel).

The capacity factor (CF) represents the ratio of the expected output power to the maximum or nominal power output P_{max}. Therefore, it can be calculated using time-averaged power output as

$$\text{CF} = \frac{\overline{P(t)}}{P_{\text{max}}} \tag{2}$$

where the overline denotes the temporal average and P_{max} is the nominal power output. If enough data is collected to construct reliable probability density functions, the capacity factor can be derived by integrating the product of the wind speed's probability density function $f_{\text{pdf}}(u)$ and the power curve $P(u)$ across all possible wind speeds:

$$\text{CF} = \frac{1}{P_{\text{max}}} \int_0^\infty f_{\text{pdf}}(u) \cdot P(u)\,\mathrm{d}u \tag{3}$$

In this study, eq. (2) was used for simplicity but also because some of the data collected were recorded over only one month, which may be insufficient to construct robust probability density functions as required by eq. (3). At each site, a reference capacity factor was calculated using lidar data. This reference was then compared to the capacity factors estimated from the wind atlases, providing a measure of the accuracy of these models in capturing the wind energy potential.

https://doi.org/10.5194/wes-2024-119
Preprint. Discussion started: 2 October 2024

eawe european academy of wind energy
Open Access WIND ENERGY SCIENCE DISCUSSIONS

4 Results

4.1 Overview of data collection

This section presents the time series data collected from lidar measurements and model databases during distinct campaigns at the five sites: FINO1 (offshore, 2015-2016), FINO3 (offshore, 2013-2014), Bjerkreim (complex terrain, 2010), Sola (coastal terrain, 2013) and Lista (coastal terrain, 2020-2021). Each time series, illustrated in fig. 6, corresponds to wind speed data collected at the height nearest to the hub height of a 15 MW offshore wind turbine at approximately 150 m. We remind that NEWA does not cover the period during which the lidar data were collected at Lista. Due to occasional data loss, lidar data series are discontinuous, and comparative analysis with model databases (NORA3, ERA5, NEWA) is restricted to periods where lidar data are available.

A qualitative analysis of the time series shows that the agreement between the lidar measurements and wind atlases is generally good, with the best match observed at the offshore sites FINO1 and FINO3 but also the coastal site Lista. At the coastal site Sola and the complex terrain Bjerkeim, NORA3 seems to perform better than NEWA and ERA5, partly because it was specifically designed for applications in Northern Europe. This direct comparison underscores the need for careful selection of wind atlases in wind resource assessment.

4.2 Error metrics across sites

Figure 7 compares four error metrics describing the discrepancies between in-situ measurements and modelled mean wind speed data across five sites: FINO1, FINO3, Sola, Bjerkreim and Lista at a single height, corresponding to the range gate of the lidar nearest to 150 m. In terms of bias, ERA5 tends to underperform in coastal and complex terrains, while NORA3, specifically developed for Norway, consistently shows the lowest bias across all the sites except at FINO1. This contrasts with earlier studies, such as those by Solbrekke et al. (2021), which reported a smaller bias with a value of 0.14 m s^{-1} at the same site. A similar bias of 0.11 m s^{-1} was obtained by Cheynet et al. (2022) for 2009 alone, both at the same site and altitude. The positive high bias observed at FINO1 during the campaign is also found when replacing the lidar data with the cup anemometer data at 100 m above sea level. This larger-than-expected bias may be attributed to the local depletion of wind resources caused by the construction of multiple wind farms around the mast since 2009. This finding is consistent with the study by Podein et al. (2022), which identified an increased wind speed bias between geostrophic wind speeds and in-situ measurements at FINO1 after 2009, coinciding with the start of wind farm development in the area.

NORA3 and ERA5 demonstrate good performance metrics for offshore sites, achieving R^2 coefficients close to 0.9, consistent with findings from Cheynet et al. (2022). In complex terrain, NORA3 surpasses NEWA and ERA5, providing the most accurate wind speed estimates as indicated by the highest R^2 coefficients, which range from 0.7 to 0.8 for NEWA and ERA5. NORA3 also provides, on average, one of the lowest RMSE across different types of terrains. Interestingly, for the two offshore sites, ERA5 marginally outperforms NORA3 in terms of RMSE. Thus, NORA3's performance is fairly consistent across diverse topographies, whereas ERA5 may be reliably applied at far offshore sites, particularly where region-specific wind atlases are not available.

https://doi.org/10.5194/wes-2024-119
Preprint. Discussion started: 2 October 2024

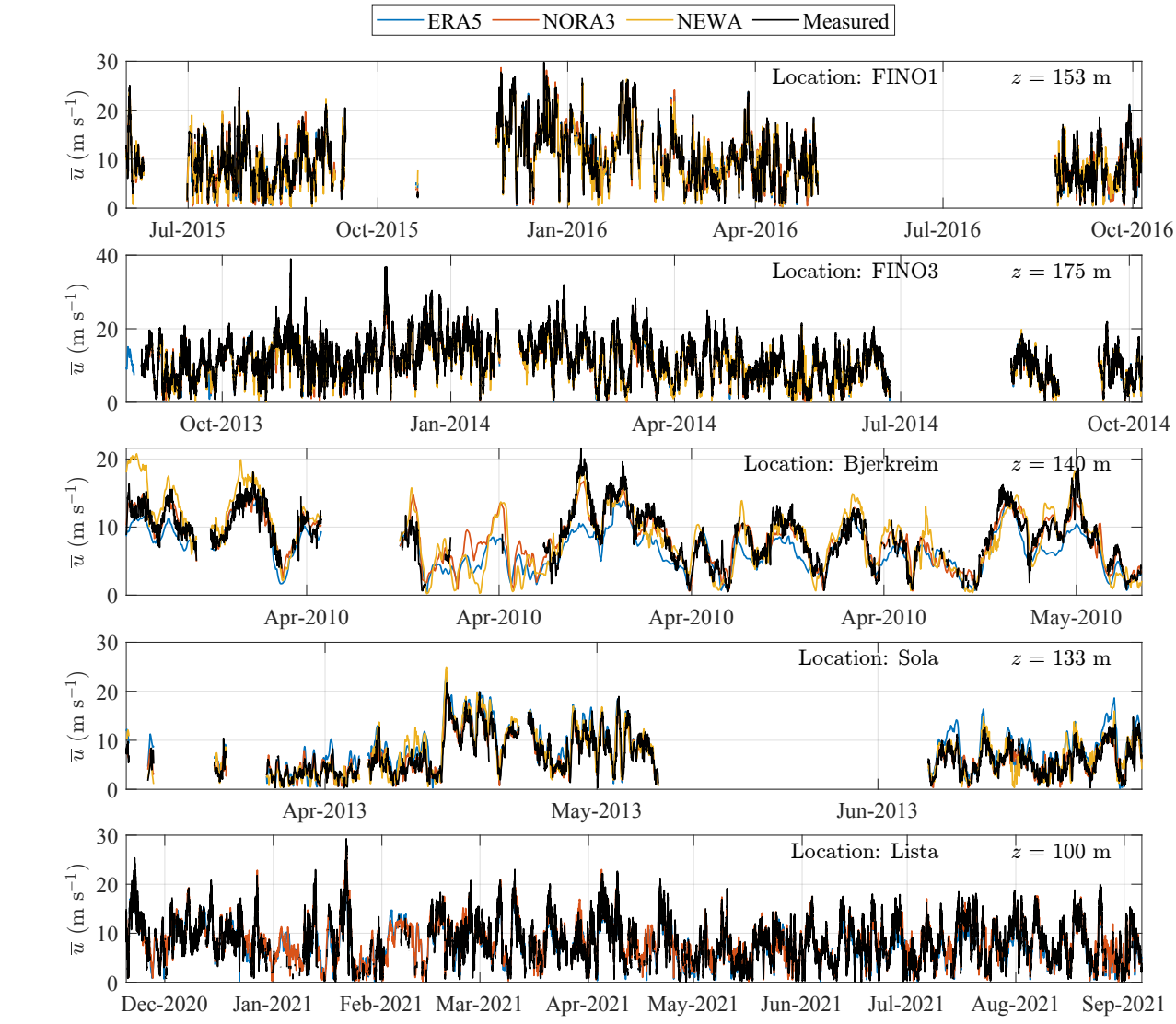

Figure 6. Time series of mean wind speed data recorded at the five reference sites (FINO1, FINO3, Bjerkreim, Sola and Lista) at the range gate nearest to 150 m. These are superposed with the corresponding time series from the ERA5, NEWA, and NORA3 databases, highlighting periods where lidar data are available.

The fourth column of fig. 7 analyses the EMD. Offshore, NEWA exhibits the lowest EMD at FINO1 and the highest at FINO3. Although NEWA was specifically engineered with this error metric in mind (Hahmann et al., 2020), the inconsistent EMD values at these two offshore sites may be attributed to the presence of multiple offshore wind farms around FINO1 at the time of data collection. At the coastal sites, the EMD values are comparable across all models, indicating similar performance among them. At the complex terrain Bjerkeim, NORA3 achieves the lowest EMD, underscoring its potential in heterogeneous topographies.

https://doi.org/10.5194/wes-2024-119
Preprint. Discussion started: 2 October 2024

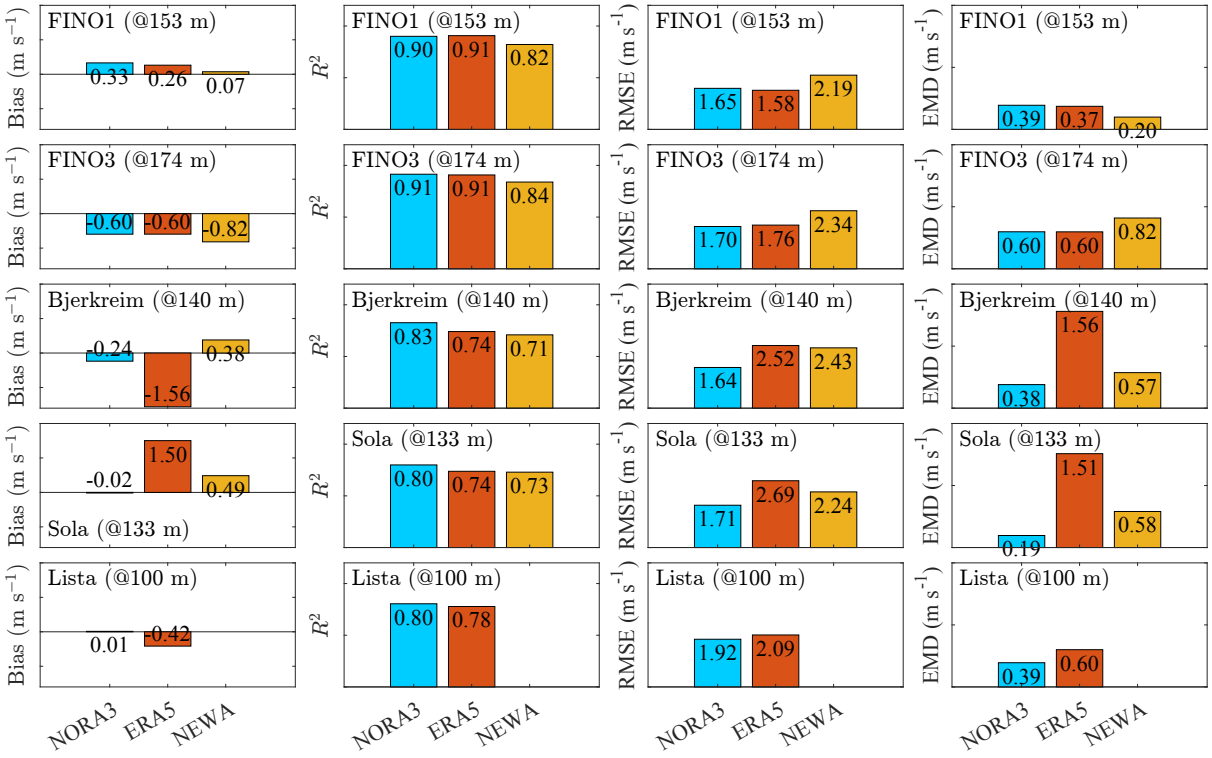

Figure 7. Comparative analysis of error metrics for in-situ measurements versus modelled mean wind speed data across the five sites (FINO1, FINO3, Sola, Bjerkreim and Lista). Each row represents one of the sites and each column represents a different error metric, arranged from left to right: Bias, R^2 Coefficient, RMSE (Root Mean Square Error), and EMD (Earth Mover's Distance).

As expected, ERA5 shows significantly higher EMD values than the other two models onshore, which is attributable to its lower horizontal spatial resolution.

The choice of the best model database is not straightforward as it depends on the specific error metrics and the location being analysed (fig. 7). Furthermore, these error metrics are influenced by the height at which measurements are taken, further challenging the selection of an optimal database for specific applications (fig. 8).

Figure 8 displays the vertical profiles or Bias, R^2 Coefficient, RMSE and EMD of the wind speed for the five sites (FINO1, FINO3, Sola, Bjerkreim and Lista) using the three model databases (NEWA, NORA3 and ERA5) at heights up to 500 m. It is reminded that the data collection was limited to up to 300 m at the complex terrain site Bjerkreim and that data from NEWA were not available during the lidar campaign at Lista. Bias profiles show generally a decrease with increasing height across the different sites, except at Bjerkreim where the results are more nuanced; NORA3's bias decreases significantly, nearing zero at higher elevations, whereas NEWA's bias increases. In contrast, ERA5's bias is strongly dependent on height. For the R^2 and RMSE metrics, NORA3 and ERA5 demonstrate closely matched results at the offshore sites FINO1 and FINO3 across all heights, likely due to NORA3's utilization of ERA5 inputs as forcing. At the coastal site Sola, NORA3 consistently surpasses

https://doi.org/10.5194/wes-2024-119
Preprint. Discussion started: 2 October 2024

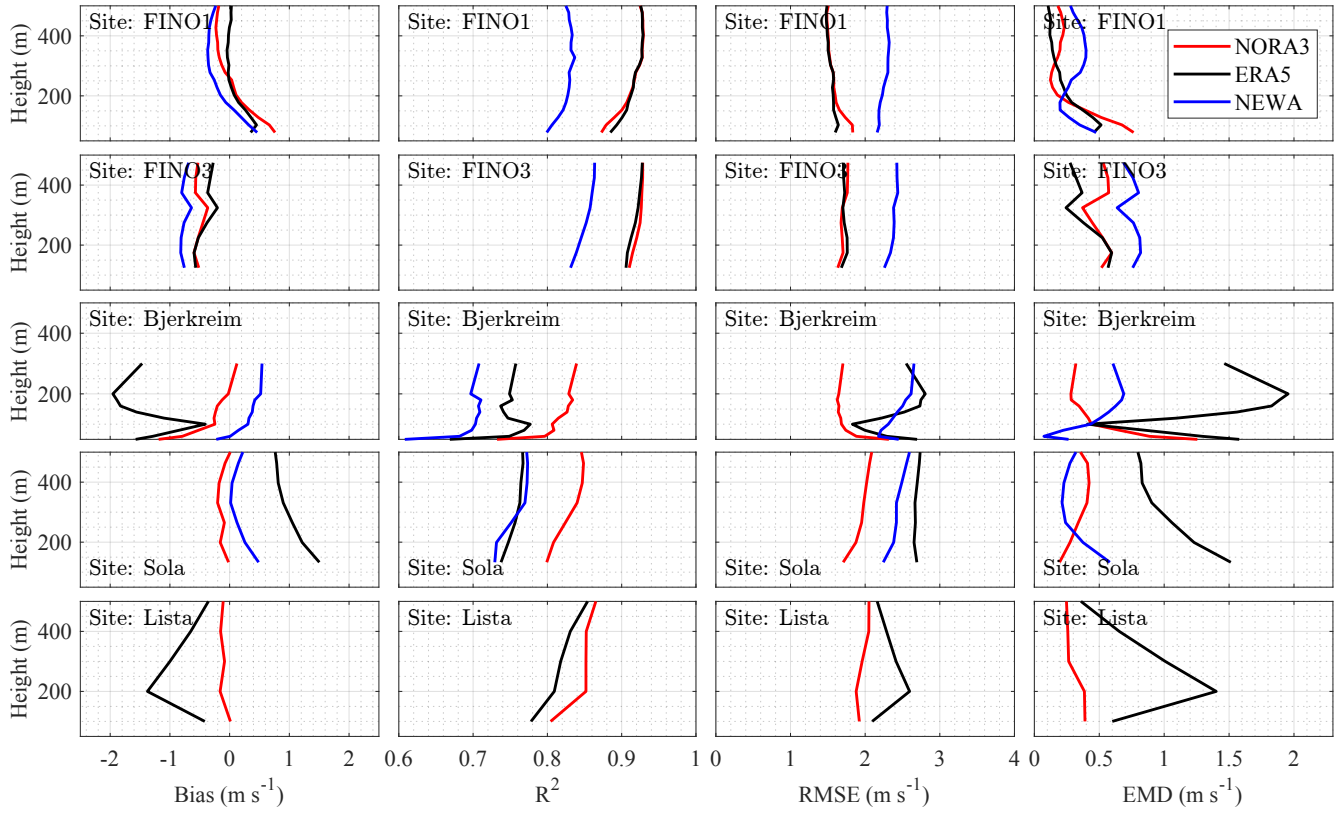

Figure 8. Comparative analysis of vertical profiles of Bias, R^2 Coefficient, RMSE (Root Mean Square Error), and EMD (Earth Mover's Distance) across the five sites: FINO1, FINO3, Sola, Bjerkreim and Lista. Each row represents one site and each column represents one error metric.

NEWA and ERA5 in R^2 values at every height. In the complex terrain of Bjerkreim, NORA3 generally exhibits the lowest RMSE. Meanwhile, NEWA and ERA5 show varying RMSE results based on height, complicating the choice of the most appropriate wind atlases for wind resource assessment.

The analysis of EMD further challenges the selection process. Offshore, ERA5 appears to be the preferred option, especially for taller wind turbines with hub heights around 150 m. In contrast, in complex terrains like Bjerkreim, NEWA performs best below 100 m but is outperformed by NORA3 at higher altitudes. The Taylor diagram shown in fig. 9 summarizes another performance assessment of the models with respect to the lidar data. This diagram visualizes the standard deviation and correlation coefficient of modelled mean wind speed data versus in-situ measurements at the five sites: FINO1, FINO3, Bjerkreim, Sola and Lista. In this figure, NORA3 usually has the best match with the measurements, especially in complex terrain and coastal areas. It performs well across various tests but ERA5 performs equally well offshore.

The selection of the most suitable wind atlases is highly contextual, depending on specific site conditions, measurement heights, and desired error metrics. ERA5 might be considered for broader applications for offshore wind energy and NEWA may

https://doi.org/10.5194/wes-2024-119
Preprint. Discussion started: 2 October 2024

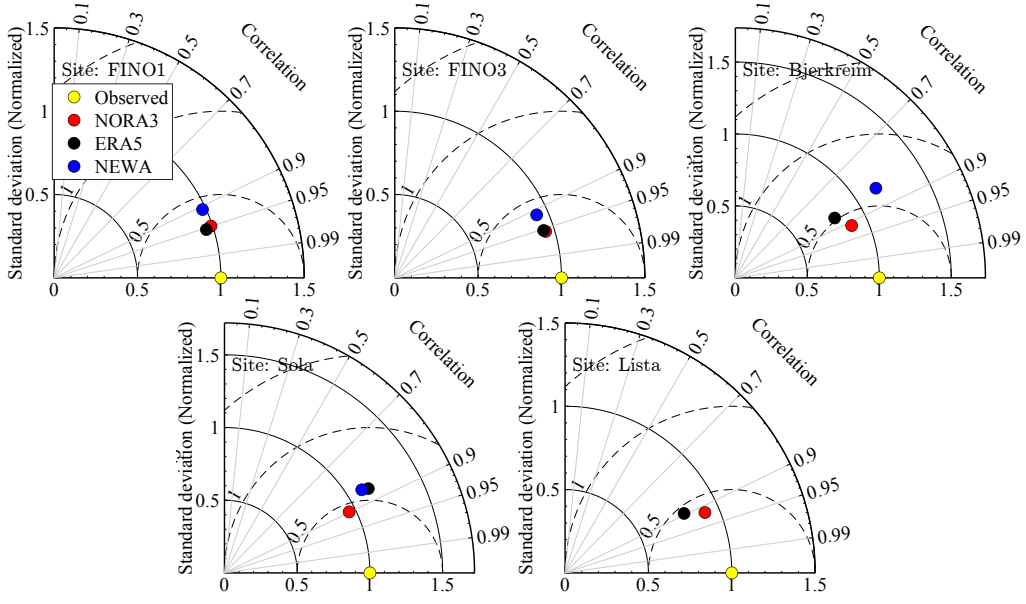

Figure 9. Taylor's diagram across the five sites: FINO1, FINO3, Bjerkreim, Sola and Lista, at a height of 150 m above the surface.

be appropriate when focusing on specific error metrics like EMD while NORA3 may deliver consistent high performance in the Norwegian onshore and offshore sites. It should also be noted that the variability in model performance across the sites may partly be attributable to the different lidar instruments used. The DWL profiler deployed in Bjerkreim in 2010 was a now-discontinued WindCube V1, whereas a scanning lidar WindCube 100S was used at the coastal site Sola and the FINO1 platform, and a discontinued WindCube WLS70 was deployed at the offshore site FINO3 and the coastal site Lista. Furthermore, each lidar's performance is inherently unique due to the fine-tuning of the hardware during the manufacturing and calibration process, the discussion of which is beyond the scope of this study.

4.3 Capacity factor estimates

This section analyses the CFs for different turbine models at the five sites. These estimates are based on the use of the time series of the wind speed measured by lidars and provided by the three wind atlases. For the case of wind turbines, each row of fig. 10 represents a specific location, while each column refers to a different turbine type. The CFs presented are not indicative of the sites' climatology, as the measurement campaigns were significantly shorter than the standard 30-year period. Also, lidars tend to have low data availability under weak wind conditions, resulting in a higher estimated CF compared to long-term, continuous measurements. Consequently, the CF here should serve solely for comparison between the model and the measurement data, and not for evaluating the wind energy potential at these sites.

The offshore site FINO3 demonstrates the best agreement between model datasets and lidar measurements in terms of CF. However, the NREL 5 MW and the IEA 15 MW wind turbines exhibit substantial differences in CF, largely due to variations in hub heights. Higher hubs capture stronger winds, which could also explain the smaller discrepancies between measured

https://doi.org/10.5194/wes-2024-119
Preprint. Discussion started: 2 October 2024

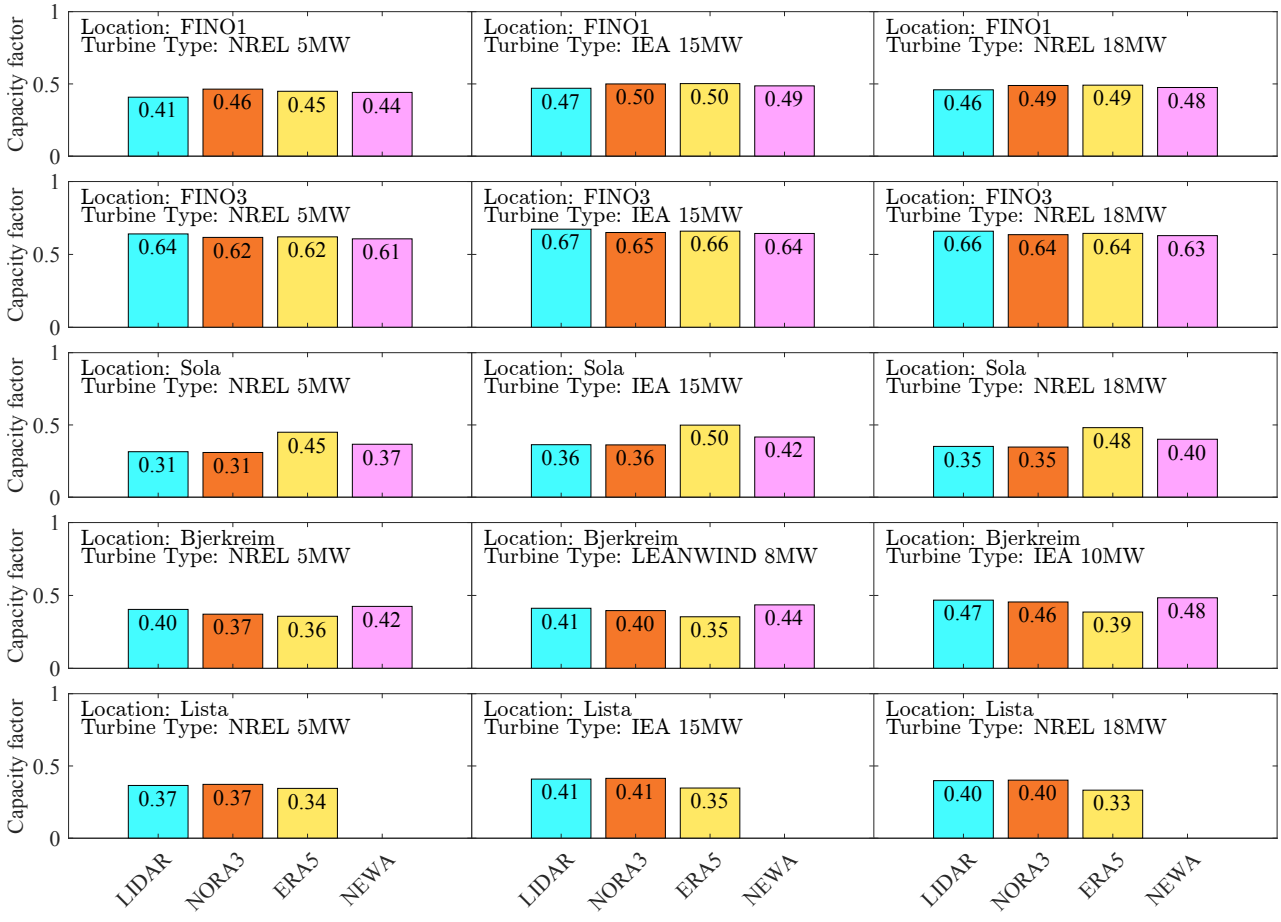

Figure 10. Estimated capacity factors for different turbine models at five sites, using lidar and three model datasets as wind inputs.

and modelled data at these altitudes. For the 15 MW wind turbines at FINO3, the estimated CFs differ by a maximum of 0.03 between measurements and ERA5. At FINO1, the discrepancies between the model and measurements are greater than at FINO3, which might be due to the presence of wind farms around the mast. These findings align with those from Figure 10, which shows decreasing discrepancies at higher altitudes in terms of bias, EMD, and correlation coefficient.

At the coastal sites Sola and Lista, the NORA3 database provides nearly identical CFs to the lidar data. In contrast, ERA5 significantly overestimates the CF by approximately 40% for the NREL 5 MW wind turbine and 38% for the IEA 15 MW wind turbine. The NEWA hindcast also overestimates the CF at Sola, though to a lesser extent: around 16% for the NREL 5 MW turbine and 14% for the IEA 15 MW turbine.

At the complex terrain site Bjerkreim, the NORA3 and ERA5 datasets slightly underestimate the CFs for the NREL 5 MW wind turbine. However, the NEWA dataset provides CFs that are closest to those measured by lidar. This finding is supported by fig. 8, which indicates that the Earth Mover's Distance (EMD), a good metric for wind resource assessment, is lower for NEWA than that for ERA5 and NORA3 below 100 m at Bjerkreim.

https://doi.org/10.5194/wes-2024-119
Preprint. Discussion started: 2 October 2024

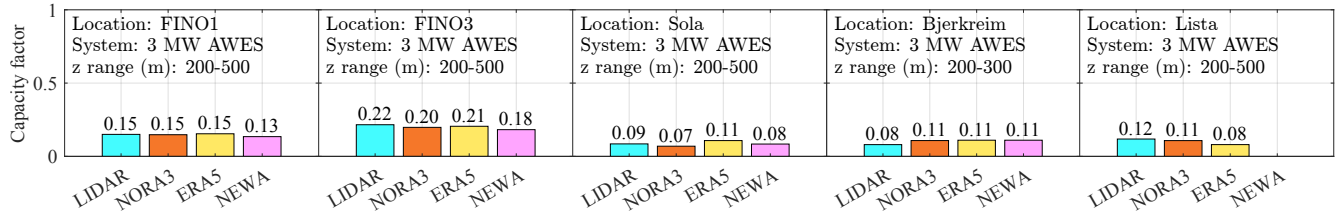

Figure 11. Estimated capacity factors for the 3 MW AWE system from Eijkelhof and Schmehl (2022) at five sites, using lidar and three wind atlases as wind inputs.

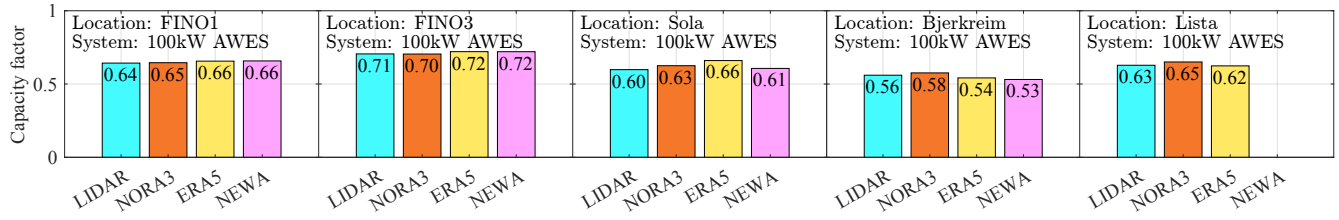

Figure 12. Estimated capacity factors for the 100 kW AWE system from Ranneberg et al. (2018) at five sites, using lidar and three wind atlases as wind inputs.

Figure 11 presents the CFs for the 3 MW AWE system, which range from 0.15 to 0.22 offshore. In contrast, fig. 12 shows CF values between 0.64 and 0.72 for the 100 kW AWE system. This significant difference is primarily due to the varying cut-in wind speeds and rated wind speeds. The 100 kW system has a cut-in wind speed of 2 m s^{-1} and a rated wind speed of approximately 7 m s^{-1}, while the 3 MW system has a cut-in wind speed of 9 m s^{-1} and a rated wind speed of 22 m s^{-1}. A less conservative power curve was used in Trevisi et al. (2021) for a 3 MW AWE system with a cut-in wind speed of 2 m s^{-1} and a rated wind speed between 7 and 8 m s^{-1}, which led to a CF $= 0.64$. Although the 3 MW system used in our study displays a higher cut-out wind speed than the 100 kW system, it does not sufficiently compensate for the lower CF. Thus, the economic success of larger AWE systems depends on incorporating lower cut-in and rated wind speeds.

Regardless of the performance differences between the two AWE systems, the CFs at the offshore sites FINO1 and FINO3 are similar when using reanalysis and lidar datasets. As noted in the previous section, NEWA slightly underestimates the CF at FINO1 and FINO3 compared to NORA3 and ERA5. The small discrepancies between simulated and lidar data at FINO1 indicate that the data are collected at sufficient altitudes to minimise the influence of local wind resource depletion due to wind farm clusters at altitudes above 200 m. For the coastal sites (Sola and Lista) and the complex terrain site (Bjerkreim), the discrepancies in CF for the 3 MW AWE system are also minor. This is likely because wind speeds below 9 m s^{-1}, which fall below the system's cut-in speed, are not included in the CF calculation. Wind atlases thus capture moderate winds more accurately than weak winds. However, deviations between the model and measurements are also documented at wind speeds above 20 m s^{-1}, either near the surface (Bentamy et al., 2021; Gandoin and Garza, 2024) or within the first 100 m above the

https://doi.org/10.5194/wes-2024-119
Preprint. Discussion started: 2 October 2024

surface (Solbrekke et al., 2021). The underperformance of wind atlases under strong wind conditions may, however, have a limited impact on the CF of wind energy systems with a relatively low cut-out speed of around 20 to 25 m s^{-1}.

While this subsection primarily examined the CF, which is directly related to the levelized cost of energy, it represents just one of several metrics used to assess the performance of intermittent renewable energy systems (Simpson et al., 2020). Alternative metrics, such as the Gini coefficient (Malz et al., 2020) and the correlation coefficient between different renewable energy sources (Malz et al., 2020; Jurasz et al., 2020), also provide valuable insights into the variability of power output in AWE systems and wind turbines. Although the tall wind speed profiles established in this study could assess the complementarity of AWE systems with other energy sources like wind and solar, such discussions fall outside the scope of this study.

5 Discussions

5.1 A need for more powerful wind profilers?

When commercial DWL profilers became available in the 2000s, wind turbines had a nominal capacity of about 5 MW, with tip heights around 150 m. This made the typical lidar scanning range of 200–300 m sufficient at the time. However, wind turbine sizes have grown significantly since then. For instance, in 2023, Mingyang Smart Energy proposed a 20 MW turbine with a tip height potentially reaching 300 m. The increasing interest in AWE systems further highlights the technical limitations of traditional lidar profilers. While scanning lidars can extend profiling range, they are often heavier, more expensive, and less reliable, as they contain more moving parts and are not specifically designed for wind profiling.

This raises concerns that the development of DWL profilers is not keeping pace with the growing size of wind turbines and AWE systems. There is a clear need for a new generation of DWL instruments capable of reliably profiling winds up to 500 m above the surface or even higher. Such instruments remain uncommon among commercial lidar producers. One notable exception is Halo Photonics by Lumibird, which has developed the BEAM 6X series, capable of measuring wind speeds up to 500 m. However, up to date we cannot find studies demonstrating the validity of measurements from this lidar.

5.2 Mesoscale limitations and microscale needs

This study primarily focuses on wind speed data derived from mesoscale models, which have certain limitations, particularly for applications in complex terrain. In offshore sites, such as FINO1 and FINO3, microscale effects may be negligible. However, in coastal sites like Sola and Lista, microscale models could improve the agreement between modelled and measured wind speeds. In complex terrain, such as at Bjerkreim, computational fluid dynamics models may be necessary to account for phenomena like flow recirculation and detached downslope flow, which are common in the mountainous terrain of Southeastern Norway. Future research should explore the potential benefits of coupling mesoscale and microscale models to improve performance metrics at the coastal and complex sites. We expect this coupling might cause the near-zero bias of NORA3 to shift toward a negative or positive value, while possibly reducing the current bias of NEWA and ERA5 toward zero. However, such an investigation falls outside the scope of this study.

https://doi.org/10.5194/wes-2024-119
Preprint. Discussion started: 2 October 2024

The comparison conducted in this study remains valuable because microscale models, while potentially more precise than mesoscale models in complex terrain, depend on accurate initial and boundary conditions that can be provided by the mesoscale models. Finally, it should be noted that the discrepancy between the modelled wind speed data and lidar-based measurements in the complex site Bjerkeim or the coastal sites Sola and Lista is not solely attributable to the lower grid resolution of the mesoscale wind model. It is also influenced by the higher occurrence of non-homogeneous flow fields at onshore sites compared to offshore, particularly within the first 300 m above the surface, which can exacerbate the measurement uncertainties of lidar retrievals using DBS or velocity-azimuth display scanning.

6 Conclusions

This study examines the capability of three state-of-the-art wind atlases, NORA3, NEWA, and ERA5, in accurately modelling wind speed profiles up to 500 m above the surface for wind energy applications. Reference wind speed profiles were obtained from Doppler wind lidar (DWL) measurements conducted at five distinct sites in Northern Europe. These sites encompass diverse topographies such as flat coastal terrain, mountainous regions, and offshore environments. The objective of the study is to broaden the validation scope to altitudes critical for large wind turbines and airborne wind energy (AWE) systems. This study addresses a significant challenge in wind energy as there has been relatively limited investigation into tall wind speed profiles using scanning DWL in profiler modes for wind resource assessment at heights up to 500 m above the surface.

The study found that all three wind atlas datasets (NORA3, NEWA, and ERA5) exhibit high quality in offshore locations, with ERA5 showing the closest correlation to lidar data up to 200 m. From 200 m to 500 m, NORA3 and ERA5 perform equally well in terms of correlation coefficient and root mean square error (RMSE), though NORA3 has a lower bias and lower earth mover's distance (EMD) above 200 m. Onshore, NORA3 outperforms ERA5 and NEWA at all heights for most error metrics. In terms of the capacity factor (CF) for large wind turbines, all datasets show good agreement with CF derived from lidar data offshore, particularly for the largest turbines. However, at the FINO1 site, CF is overestimated by all models, likely due to local wind resource depletion from surrounding offshore wind farms. In coastal terrain, NORA3 provides excellent CF agreement with lidar data, NEWA performs reasonably well, but ERA5 overestimates the CF. In complex terrain, NEWA and NORA3 both perform well, while ERA5 substantially underestimates the CF. For AWE systems, the CF was fairly consistent across all the wind atlases but showed considerable dependency on the power curve. In particular, the efficiency of the larger 3 MW AWE system considered in this study is penalized by a high cut-in and rated wind speed compared to the smaller 100 kW system.

It should be noted that this study was conducted using relatively limited datasets, which do not cover a climatology timescale and include measurements from a few locations in Norway and the North Sea. Although the sites selected in this study provide a diverse range of topographies, having more locations from additional countries would enhance the robustness of the findings. Additionally, the limited temporal resolution of the dataset may not fully capture short-term variability in wind speed profiles, which needs to be considered in regions where non-stationary boundary layers are prevalent.

The general conclusion is that NORA3 excels onshore, while ERA5, with its global coverage, performs equally well offshore. Onshore data quality is slightly lower across all datasets due to the complexity of wind patterns over land, with ERA5 showing

https://doi.org/10.5194/wes-2024-119
Preprint. Discussion started: 2 October 2024

eawe european academy of wind energy
Open Access WIND ENERGY SCIENCE DISCUSSIONS

significant height-dependent errors, possibly due to inaccuracies in geopotential height and pressure level data over mountainous terrain. These findings underscore the importance of selecting the appropriate wind atlas for specific sites and altitudes to enhance wind speed predictions and wind energy estimates. Performance variations across different locations and heights highlight the need for tailored wind resource assessments, especially in complex terrains. Smaller AWE systems with lower cut-in and rated wind speeds achieve higher CFs and efficiency compared to multi-megawatt systems. Therefore, designing larger AWE systems with low cut-in wind speeds is crucial for broader adoption. Finally, the development of DWL profiler technology must keep pace with the growing size of wind turbines, requiring more powerful profilers to avoid the higher costs associated with the use of scanning lidar instruments for tall wind profiles.

Appendix A: Error metrics with non-linear wind speed regression

A non-linear regression was also tested instead of an interpolation for smoothing the vertical wind speed profiles up to 500 m above the surface for NEWA and NORA3 and for the first six height levels for ERA5. The regression relies on fitting a modification of the wind profile model by Deaves and Harris (1982). This modified analytical function combines a classic logarithmic profile with a third-order polynomial function and is expressed as

$$\overline{u}(z) = \frac{u_*}{\kappa} \log\left(\frac{z}{z_0}\right) + p(z), \text{ with} \tag{A1}$$

$$p(z) = a_1(z) + a_2(z)^2 + a_3(z)^3, \tag{A2}$$

where z is the height above the surface; $\kappa \approx 0.4$ is the von Kármán constant and z_0 is the roughness length. The coefficients a_i, where $i = \{1,2,3\}$, are determined empirically by least-squares fit (Cheynet et al., 2024). For the coastal and complex terrain sites, the roughness length is approximated by the values 0.01 m and 0.1 m, respectively, following the traditional roughness length classification onshore (Wieringa, 1980, 1986). These values are realistic enough to ensure a reasonable fit in the lower part of the atmospheric boundary layer. Above the ocean, the roughness length is estimated using Charnock's relationship, which quantifies the dependency of the roughness length on the sea state (Charnock, 1955):

$$z_0 = \frac{a}{g} u_*^2 \tag{A3}$$

where $g = 9.81\,\mathrm{ms}^{-2}$ is the gravitational acceleration, and $a \approx 0.014$ is an empirical coefficient (Kraus and Businger, 1994). Equation (A3) is combined with the neutral logarithmic wind speed profile into a new equation:

$$z_0 - \frac{a}{g}\left[\frac{\kappa \overline{u}(z_r)}{\ln(z_r/z_0)}\right]^2 = 0, \tag{A4}$$

which is solved for $z_r = 10$ m and provides an estimate of the roughness length in the marine atmospheric boundary layer.

Figure A1 and fig. A2 present the error metrics used to assess the performance of the wind atlases compared to lidar measurements, based on wind speed data, at a specific height and up to 500 m across the five investigated sites, respectively. The non-linear regression produces profiles of error metrics that show less variance around their mean but does not necessarily

https://doi.org/10.5194/wes-2024-119
Preprint. Discussion started: 2 October 2024

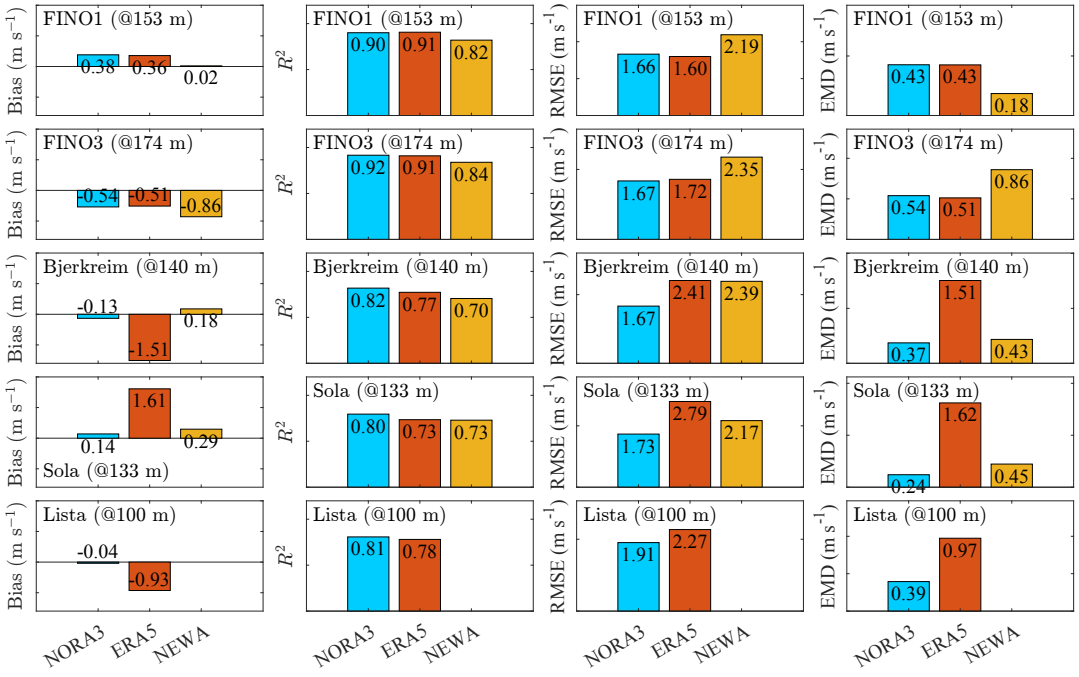

Figure A1. Comparative analysis of error metrics for in-situ measurements versus modelled mean wind speed data across the five sites (FINO1, FINO3, Sola, Bjerkreim and Lista). Each row represents one site and each column represents a different error metric, arranged from left to right: Bias, R^2 Coefficient, RMSE (Root Mean Square Error), and EMD (Earth Mover's Distance). The spatial collocation was obtained by non-linear regression instead of linear interpolation.

reduce the error metrics themselves. Several hundreds or thousands of samples are used to compute these ensemble-averaged error metrics, which tend to smooth out possible discrepancies due to linear interpolation. Therefore, when sufficiently large datasets are available, linear interpolation of the vertical wind speed profiles at additional height levels produces good results and was found to be the most reliable approach in this study.

Data availability. The datasets used to generate the figures in this study will be made publicly available on Zenodo under a BSD-3 open-access license.

Author contributions. JR, JMD, HH and ØB contributed to the conceptualization of the study. EC, JMD, and JR developed the methodology. Data collection was carried out by EC, JMD, JR, and AP, while data analysis was performed by EC and JMD. The original draft was written by EC and JMD, and all authors participated in the review and editing process. Supervision was provided by JR and EC, and JR was responsible for funding acquisition.

https://doi.org/10.5194/wes-2024-119
Preprint. Discussion started: 2 October 2024

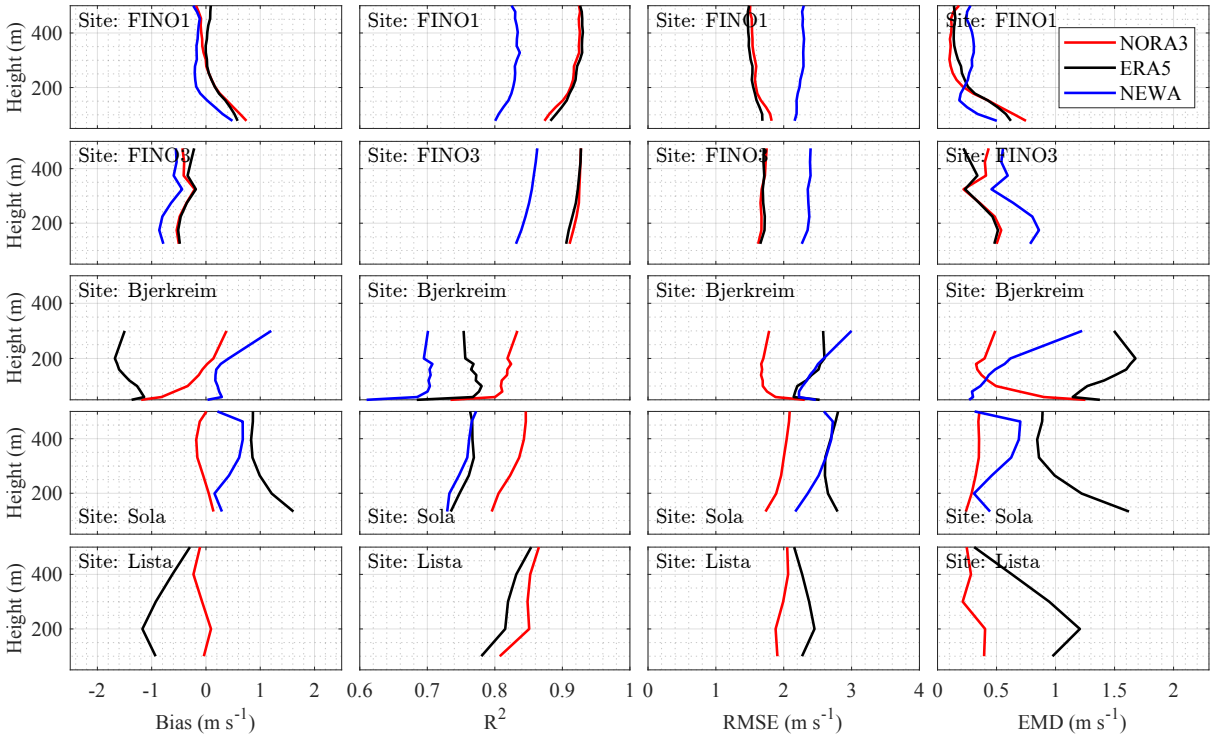

Figure A2. Comparative analysis of vertical profiles based on non-linear regression for Bias, R^2 Coefficient, RMSE (Root Mean Square Error), and EMD (Earth Mover's Distance) across the five sites: FINO1, FINO3, Sola, Bjerkreim and Lista. Each row represents one site and each column represents one error metric.

Competing interests. Etienne Cheynet and Alfredo Peña are members of the editorial board of Wind Energy Science.

Acknowledgements. This work is co-funded by the European Union's Horizon 2020 research and innovation program under the Marie Sklodowska-Curie grant agreement No. 858358 (LIKE –Lidar Knowledge Europe, H2020-MSCA-ITN-2019), the projects Large Offshore Wind Turbines (LOWT) (project number: 325294) and ImpactWind Southwest (project number: 332034) funded by the Research Council of Norway and the Marie Sklodowska-Curie grant agreement No. 101168855 (NEXTgenT - NEXT generation of over 25MW offshore wind Turbine rotor design, HORIZON-MSCA-2023-DN-01).

https://doi.org/10.5194/wes-2024-119
Preprint. Discussion started: 2 October 2024

eawe european academy of wind energy
Open Access WIND ENERGY SCIENCE DISCUSSIONS

References

Akima, H.: A method of bivariate interpolation and smooth surface fitting based on local procedures, Communications of the ACM, 17, 18–20, 1974.

Amidror, I.: Scattered data interpolation methods for electronic imaging systems: a survey, Journal of Electronic Imaging, 11, 157–176, 2002.

Antonini, E. G., Virgüez, E., Ashfaq, S., Duan, L., Ruggles, T. H., and Caldeira, K.: Identification of reliable locations for wind power generation through a global analysis of wind droughts, Communications Earth & Environment, 5, 1–9, 2024.

Banta, R. M., Pichugina, Y. L., Kelley, N. D., Hardesty, R. M., and Brewer, W. A.: Wind energy meteorology: Insight into wind properties in the turbine-rotor layer of the atmosphere from high-resolution Doppler lidar, Bulletin of the American Meteorological Society, 94, 883–902, 2013.

Beck, H. and Kühn, M.: Dynamic data filtering of long-range Doppler LiDAR wind speed measurements, Remote Sensing, 9, 561, 2017.

Bentamy, A., Grodsky, S. A., Cambon, G., Tandeo, P., Capet, X., Roy, C., Herbette, S., and Grouazel, A.: Twenty-Seven years of scatterometer surface wind analysis over eastern boundary upwelling systems, Remote Sensing, 13, 940, 2021.

Cariou, J., Boquet, M., Lolli, S., Parmentier, R., and Sauvage, L.: Validation of the new long range 1.5 μm wind lidar WLS70 for atmospheric dynamics studies, in: Lidar Technologies, Techniques, and Measurements for Atmospheric Remote Sensing V, vol. 7479, pp. 180–189, SPIE, 2009.

Charnock, H.: Wind stress on a water surface, Quarterly Journal of the Royal Meteorological Society, 81, 639–640, 1955.

Chen, W.-B.: Analysing seven decades of global wave power trends: The impact of prolonged ocean warming, Applied Energy, 356, 122 440, 2024.

Cheynet, E., Jakobsen, J. B., Snæbjörnsson, J., Reuder, J., Kumer, V., and Svardal, B.: Assessing the potential of a commercial pulsed lidar for wind characterisation at a bridge site, Journal of Wind Engineering and Industrial Aerodynamics, 161, 17–26, 2017.

Cheynet, E., Flügge, M., Reuder, J., Jakobsen, J. B., Heggelund, Y., Svardal, B., Saavedra Garfias, P., Obhrai, C., Daniotti, N., Berge, J., et al.: The COTUR project: remote sensing of offshore turbulence for wind energy application, Atmospheric Measurement Techniques, 14, 6137–6157, 2021.

Cheynet, E., Solbrekke, I. M., Diezel, J. M., and Reuder, J.: A one-year comparison of new wind atlases over the North Sea, in: Journal of Physics: Conference Series, vol. 2362, p. 012009, IOP Publishing, 2022.

Cheynet, E., Li, L., and Jiang, Z.: Metocean conditions at two Norwegian sites for development of offshore wind farms, Renewable Energy, 224, 120 184, 2024.

Davis, E. V., Rajeev, K., and Mishra, M. K.: Effect of clouds on the diurnal evolution of the atmospheric boundary-layer height over a tropical coastal station, Boundary-Layer Meteorology, 175, 135–152, 2020.

Davis, E. V., Rajeev, K., and Sambhu Namboodiri, K.: The convective-atmospheric-boundary-layer height and its dependence upon meteorological variables at a tropical coastal station during onshore and offshore flows, Boundary-Layer Meteorology, 183, 143–166, 2022.

Deaves, D. and Harris, R.: A note on the use of asymptotic similarity theory in neutral atmospheric boundary layers, Atmospheric Environment, 16, 1889–1893, 1982.

Dee, D. P., Uppala, S. M., Simmons, A. J., Berrisford, P., Poli, P., Kobayashi, S., Andrae, U., Balmaseda, M., Balsamo, G., Bauer, d. P., et al.: The ERA-Interim reanalysis: Configuration and performance of the data assimilation system, Quarterly Journal of the Royal Meteorological Society, 137, 553–597, 2011.

https://doi.org/10.5194/wes-2024-119
Preprint. Discussion started: 2 October 2024

Dias Neto, J., Nuijens, L., Unal, C., and Knoop, S.: Combined wind lidar and cloud radar for high-resolution wind profiling, Earth System Science Data, 15, 769–789, 2023.

Dörenkämper, M., Olsen, B. T., Witha, B., Hahmann, A. N., Davis, N. N., Barcons, J., Ezber, Y., García-Bustamante, E., González-Rouco, J. F., Navarro, J., et al.: The making of the new european wind atlas–part 2: Production and evaluation, Geoscientific Model Development, 13, 5079–5102, 2020.

Duscha, C., Pálenik, J., Spengler, T., and Reuder, J.: Observing atmospheric convection with dual-scanning lidars, Atmospheric Measurement Techniques, 16, 5103–5123, 2023.

Egger, J., Bajrachaya, S., Heinrich, R., Kolb, P., Lämmlein, S., Mech, M., Reuder, J., Schäper, W., Shakya, P., Schween, J., et al.: Diurnal winds in the Himalayan Kali Gandaki valley. Part III: Remotely piloted aircraft soundings, Monthly Weather Review, 130, 2042–2058, 2002.

Eijkelhof, D. and Schmehl, R.: Six-degrees-of-freedom simulation model for future multi-megawatt airborne wind energy systems, Renewable Energy, 196, 137–150, 2022.

Fagiano, L., Quack, M., Bauer, F., Carnel, L., and Oland, E.: Autonomous airborne wind energy systems: accomplishments and challenges, Annual Review of Control, Robotics, and Autonomous Systems, 5, 603–631, 2022.

Furevik, B. R. and Haakenstad, H.: Near-surface marine wind profiles from rawinsonde and NORA10 hindcast, Journal of Geophysical Research: Atmospheres, 117, 2012.

Gandoin, R. and Garza, J.: Underestimation of strong wind speeds offshore in ERA5: evidence, discussion and correction, Wind Energy Science, 9, 1727–1745, https://doi.org/10.5194/wes-9-1727-2024, 2024.

Giard, D. and Bazile, E.: Implementation of a new assimilation scheme for soil and surface variables in a global NWP model, Monthly weather review, 128, 997–1015, https://doi.org/10.1175/1520-0493(2000)128<0973:ACAOMS>2.0.CO;2, 2000.

Gottschall, J., Gribben, B., Stein, D., and Würth, I.: Floating lidar as an advanced offshore wind speed measurement technique: current technology status and gap analysis in regard to full maturity, Wiley Interdisciplinary Reviews: Energy and Environment, 6, e250, 2017.

Gualtieri, G.: Reliability of ERA5 reanalysis data for wind resource assessment: a comparison against tall towers, Energies, 14, 4169, 2021.

Haakenstad, H., Breivik, Ø., Furevik, B. R., Reistad, M., Bohlinger, P., and Aarnes, O. J.: NORA3: A Nonhydrostatic High-Resolution Hindcast of the North Sea, the Norwegian Sea, and the Barents Sea, Journal of Applied Meteorology and Climatology, 60, 1443–1464, 2021.

Hahmann, A. N., Sīle, T., Witha, B., Davis, N. N., Dörenkämper, M., Ezber, Y., García-Bustamante, E., González-Rouco, J. F., Navarro, J., Olsen, B. T., et al.: The making of the New European Wind Atlas–part 1: model sensitivity, Geoscientific Model Development, 13, 5053–5078, 2020.

Hallgren, C., Aird, J. A., Ivanell, S., Körnich, H., Vakkari, V., Barthelmie, R. J., Pryor, S. C., and Sahlée, E.: Machine learning methods to improve spatial predictions of coastal wind speed profiles and low-level jets using single-level ERA5 data, Wind Energy Science, 9, 821–840, https://doi.org/10.5194/wes-9-821-2024, 2024.

Hayes, L., Stocks, M., and Blakers, A.: Accurate long-term power generation model for offshore wind farms in Europe using ERA5 reanalysis, Energy, 229, 120 603, 2021.

Hersbach, H., Bell, B., Berrisford, P., Hirahara, S., Horányi, A., Muñoz-Sabater, J., Nicolas, J., Peubey, C., Radu, R., Schepers, D., et al.: The ERA5 global reanalysis, Quarterly Journal of the Royal Meteorological Society, 146, 1999–2049, 2020.

IEC: Wind turbines – Part 1: Design requirements, International Electrotechnical Commission, 3 edn., available from: IEC, [URL or place where it can be accessed], 2005.

https://doi.org/10.5194/wes-2024-119
Preprint. Discussion started: 2 October 2024

Jahani, K., Langlois, R. G., and Afagh, F. F.: Structural dynamics of offshore Wind Turbines: A review, Ocean Engineering, 251, 111 136, 2022.

Jiang, Z.: Installation of offshore wind turbines: A technical review, Renewable and Sustainable Energy Reviews, 139, 110 576, 2021.

Jourdier, B.: Evaluation of ERA5, MERRA-2, COSMO-REA6, NEWA and AROME to simulate wind power production over France, Advances in Science and Research, 17, 63–77, https://doi.org/10.5194/asr-17-63-2020, 2020.

Jurasz, J., Canales, F., Kies, A., Guezgouz, M., and Beluco, A.: A review on the complementarity of renewable energy sources: Concept, metrics, application and future research directions, Solar Energy, 195, 703–724, 2020.

Kelly, M., Troen, I., and Jørgensen, H. E.: Weibull-k revisited:"tall" profiles and height variation of wind statistics, Boundary-Layer Meteorology, 152, 107–124, 2014.

Kent, C. W., Grimmond, C. S. B., Gatey, D., and Barlow, J. F.: Assessing methods to extrapolate the vertical wind-speed profile from surface observations in a city centre during strong winds, Journal of Wind Engineering and Industrial Aerodynamics, 173, 100–111, 2018.

Knoop, S., Ramakrishnan, P., and Wijnant, I.: Dutch Offshore Wind Atlas Validation against Cabauw Meteomast Wind Measurements, Energies, 13, 6558, 2020.

Knoop, S., Bosveld, F. C., de Haij, M. J., and Apituley, A.: A 2-year intercomparison of continuous-wave focusing wind lidar and tall mast wind measurements at Cabauw, Atmospheric Measurement Techniques, 14, 2219–2235, 2021.

Kraus, E. B. and Businger, J. A.: Atmosphere-ocean interaction, vol. 27, Oxford University Press, 1994.

Krishnamurthy, R., Choukulkar, A., Calhoun, R., Fine, J., Oliver, A., and Barr, K.: Coherent Doppler lidar for wind farm characterization, Wind Energy, 16, 189–206, 2013.

Kruijff, M. and Ruiterkamp, R.: A Roadmap Towards Airborne Wind Energy in the Utility Sector, pp. 643–662, Springer Singapore, Singapore, https://doi.org/10.1007/978-981-10-1947-0_26, 2018.

Kumer, V. M., Reuder, J., and Furevik, B. R.: A comparison of LiDAR and radiosonde wind measurements, Energy Procedia, 53, 214–220, https://doi.org/10.1016/j.egypro.2014.07.230, 2014.

Kumer, V.-M., Reuder, J., Dorninger, M., Zauner, R., and Grubišić, V.: Turbulent kinetic energy estimates from profiling wind LiDAR measurements and their potential for wind energy applications, Renewable Energy, 99, 898–910, 2016.

Malz, E., Hedenus, F., Göransson, L., Verendel, V., and Gros, S.: Drag-mode airborne wind energy vs. wind turbines: An analysis of power production, variability and geography, Energy, 193, 116 765, 2020.

Mariani, Z., Crawford, R., Casati, B., and Lemay, F.: A multi-year evaluation of Doppler lidar wind-profile observations in the Arctic, Remote Sensing, 12, 323, 2020.

Martinez, A. and Iglesias, G.: Global wind energy resources decline under climate change, Energy, 288, 129 765, 2024.

Mason, P. and Derbyshire, S.: Large-eddy simulation of the stably-stratified atmospheric boundary layer, Boundary-layer meteorology, 53, 117–162, 1990.

Olauson, J.: ERA5: The new champion of wind power modelling?, Renewable Energy, 126, 322–331, 2018.

Pal, S. and Lee, T. R.: Contrasting air mass advection explains significant differences in boundary layer depth seasonal cycles under onshore versus offshore flows, Geophysical Research Letters, 46, 2846–2853, 2019.

Palomaki, R. T., Rose, N. T., van den Bossche, M., Sherman, T. J., and De Wekker, S. F.: Wind estimation in the lower atmosphere using multirotor aircraft, Journal of Atmospheric and Oceanic Technology, 34, 1183–1191, https://doi.org/10.1175/JTECH-D-16-0177.1, 2017.

Päschke, E., Leinweber, R., and Lehmann, V.: An assessment of the performance of a 1.5 μm Doppler lidar for operational vertical wind profiling based on a 1-year trial, Atmospheric Measurement Techniques, 8, 2251–2266, 2015.

https://doi.org/10.5194/wes-2024-119
Preprint. Discussion started: 2 October 2024

Pauscher, L., Vasiljevic, N., Callies, D., Lea, G., Mann, J., Klaas, T., Hieronimus, J., Gottschall, J., Schwesig, A., Kühn, M., et al.: An inter-comparison study of multi-and DBS lidar measurements in complex terrain, Remote Sensing, 8, 782, 2016.

Peña, A., Hasager, C. B., Gryning, S.-E., Courtney, M., Antoniou, I., and Mikkelsen, T.: Offshore wind profiling using light detection and ranging measurements, Wind Energy, 12, 105–124, 2009.

Peña, A., Gryning, S. E., and Floors, R.: Lidar observations of marine boundary-layer winds and heights: A preliminary study, Meteorologische Zeitschrift, 24, 581–589, https://doi.org/10.1127/metz/2015/0636, 2015.

Peña, A., Mann, J., Angelou, N., and Jacobsen, A.: A Motion-Correction Method for Turbulence Estimates from Floating Lidars, Remote Sensing, 14, 6065, 2022.

Pichugina, Y. L., Banta, R. M., Brewer, W. A., Sandberg, S. P., and Hardesty, R. M.: Doppler lidar–based wind-profile measurement system for offshore wind-energy and other marine boundary layer applications, Journal of Applied Meteorology and Climatology, 51, 327–349, 2012.

Podein, P., Tinz, B., Blender, R., and Detels, T.: Reconstruction of annual mean wind speed statistics at 100 m height of FINO1 and FINO2 masts with reanalyses and the geostrophic wind, Meteorologische Zeitschrift, 31, 89–100, 2022.

Pronk, V., Bodini, N., Optis, M., Lundquist, J. K., Moriarty, P., Draxl, C., Purkayastha, A., and Young, E.: Can reanalysis products outperform mesoscale numerical weather prediction models in modeling the wind resource in simple terrain?, Wind Energy Science, 7, 487–504, 2022.

Radnoti, G.: Comments on a spectral limited-area formulation with time dependent boundary conditions applied to the shallow water equations, Mon. Weather Rev., 123, 3122–3123, https://doi.org/https://doi.org/b83s7b, 1995.

Ramon, J., Lledó, L., Torralba, V., Soret, A., and Doblas-Reyes, F. J.: What global reanalysis best represents near-surface winds?, Quarterly Journal of the Royal Meteorological Society, 145, 3236–3251, 2019.

Ramon, J., Lledó, L., Pérez-Zanón, N., Soret, A., and Doblas-Reyes, F. J.: The Tall Tower Dataset: a unique initiative to boost wind energy research, Earth System Science Data, 12, 429–439, 2020.

Ranneberg, M., Wölfle, D., Bormann, A., Rohde, P., Breipohl, F., and Bastigkeit, I.: Fast Power Curve and Yield Estimation of Pumping Airborne Wind Energy Systems, pp. 623–641, Springer Singapore, 2018.

Reuder, J., Brisset, P., Jonassen, M., Müller, M., and Mayer, S.: The Small Unmanned Meteorological Observer SUMO: A new tool for atmospheric boundary layer research, Meteorologische Zeitschrift, 18, 141–147, https://doi.org/10.1127/0941-2948/2009/0363, 2009.

Reuder, J., Flügge, M., Paskyabi, M. B., Cheynet, E., Duscha, C., Kral, S. T., Garfias, P. S., Fer, I., Svardal, B., Frühmann, R., Jakobsen, J. B., Wagner, D., Fligg, A., Külpmann, A., von Bremen, L., Gottschall, J., Kreklau, M., Hahn, J., Outzen, O., Herklotz, K., and Gellatly, B.: OBLEX-F1: An Extensive Observational Effort for Offshore Wind Energy Research with Emphasis on Atmospheric Measurements, Under preparation, 2024.

Rubio, H., Kühn, M., and Gottschall, J.: Evaluation of low-level jets in the southern Baltic Sea: a comparison between ship-based lidar observational data and numerical models, Wind Energy Science, 7, 2433–2455, https://doi.org/10.5194/wes-7-2433-2022, 2022.

Schelbergen, M., Kalverla, P. C., Schmehl, R., and Watson, S. J.: Clustering wind profile shapes to estimate airborne wind energy production, Wind Energy Science, 5, 1097–1120, https://doi.org/10.5194/wes-5-1097-2020, 2020.

Shaw, W. J., Berg, L. K., Debnath, M., Deskos, G., Draxl, C., Ghate, V. P., Hasager, C. B., Kotamarthi, R., Mirocha, J. D., Muradyan, P., et al.: Scientific challenges to characterizing the wind resource in the marine atmospheric boundary layer, Wind Energy Science, 7, 2307–2334, 2022.

Shimura, T., Inoue, M., Tsujimoto, H., Sasaki, K., and Iguchi, M.: Estimation of Wind Vector Profile Using a Hexarotor Unmanned Aerial Vehicle and Its Application to Meteorological Observation up to 1000 m above Surface, Journal of Atmospheric and Oceanic Technology, 35, 1621–1631, https://doi.org/10.1175/JTECH-D-17-0186.1, 2018.

https://doi.org/10.5194/wes-2024-119
Preprint. Discussion started: 2 October 2024

Simpson, J., Loth, E., and Dykes, K.: Cost of Valued Energy for design of renewable energy systems, Renewable Energy, 153, 290–300, 2020.

Smith, D. A., Harris, M., Coffey, A. S., Mikkelsen, T., Jørgensen, H. E., Mann, J., and Danielian, R.: Wind lidar evaluation at the Danish wind test site in Høvsøre, Wind Energy, 9, 87–93, 2006.

Solbrekke, I. M., Sorteberg, A., and Haakenstad, H.: The 3 km Norwegian reanalysis (NORA3)–a validation of offshore wind resources in the North Sea and the Norwegian Sea, Wind Energy Science, 6, 1501–1519, 2021.

Sommerfeld, M., Crawford, C., Monahan, A., and Bastigkeit, I.: LiDAR-based characterization of mid-altitude wind conditions for airborne wind energy systems, Wind Energy, 22, 1101–1120, 2019a.

Sommerfeld, M., Dörenkämper, M., Steinfeld, G., and Crawford, C.: Improving mesoscale wind speed forecasts using lidar-based observation nudging for airborne wind energy systems, Wind energy science, 4, 563–580, 2019b.

Sommerfeld, M., Dörenkämper, M., De Schutter, J., and Crawford, C.: Impact of wind profiles on ground-generation airborne wind energy system performance, Wind Energy Science, 8, 1153–1178, 2023.

Taillefer, F.: CANARI - Technical documentation - Based on ARPEGE cycle CY25T1, Tech. rep., Météo-France, CNRM/GMAP, 2002.

Termonia, P., Fischer, C., Bazile, E., Bouyssel, F., Brožková, R., Bénard, P., Bochenek, B., Degrauwe, D., Derková, M., El Khatib, R., et al.: The ALADIN System and its canonical model configurations AROME CY41T1 and ALARO CY40T1, Geoscientific Model Development, 11, 257–281, 2018.

Tieo, J.-J., Skote, M., and Srikanth, N.: Suitability of power-law extrapolation for wind speed estimation on a tropical island, Journal of Wind Engineering and Industrial Aerodynamics, 205, 104 317, 2020.

Trevisi, F., McWilliam, M., and Gaunaa, M.: Configuration optimization and global sensitivity analysis of ground-gen and fly-gen airborne wind energy systems, Renewable Energy, 178, 385–402, 2021.

Valldecabres, L., Diaz, A. P., Courtney, M., von Bremen, L., and Kühn, M.: Very short-term forecast of near-coastal flow using scanning lidars, Wind Energy Science, 3, 313–327, 2018.

Vasiljevic, N.: A time-space synchronization of coherent Doppler scanning lidars for 3D measurements of wind fields, Phd thesis, DTU Wind Energy, 2014.

Veers, P., Dykes, K., Lantz, E., Barth, S., Bottasso, C. L., Carlson, O., Clifton, A., Green, J., Green, P., Holttinen, H., et al.: Grand challenges in the science of wind energy, Science, 366, eaau2027, 2019.

Vermillion, C., Cobb, M., Fagiano, L., Leuthold, R., Diehl, M., Smith, R. S., Wood, T. A., Rapp, S., Schmehl, R., Olinger, D., et al.: Electricity in the air: Insights from two decades of advanced control research and experimental flight testing of airborne wind energy systems, Annual Reviews in Control, 52, 330–357, 2021.

Vos, H., Lombardi, F., Joshi, R., Schmehl, R., and Pfenninger, S.: The potential role of airborne and floating wind in the North Sea region, Environmental Research: Energy, 1, 025 002, 2024.

Wieringa, J.: Representativeness of wind observations at airports, Bulletin of the American Meteorological Society, 61, 962–971, 1980.

Wieringa, J.: Roughness-dependent geographical interpolation of surface wind speed averages, Quarterly Journal of the Royal Meteorological Society, 112, 867–889, 1986.

Wiser, R., Millstein, D., Bolinger, M., Jeong, S., and Mills, A.: The hidden value of large-rotor, tall-tower wind turbines in the United States, Wind Engineering, 45, 857–871, 2021.

Zemba, J. and Friehe, C. A.: The marine atmospheric boundary layer jet in the Coastal Ocean Dynamics Experiment, Journal of Geophysical Research: Oceans, 92, 1489–1496, 1987.